An oceanic mechanism for glacial greenhouse gas fluctuations

Andreas Schmittner, College of Oceanic and Atmospheric Sciences, Oregon State University.

Eric D. Galbraith, Atmospheric and Ocean Sciences, Princeton University.

Earth's climate and atmospheric greenhouse gases varied dramatically on millennial time scales during past glacial periods, providing an important test bed for understanding the dynamical links that will control the response of the Earth system to ongoing and future anthropogenic perturbations. The Dansgaard-Oeschger (D-O) oscillations were characterized by coupled, but contrasting, temperature changes in Greenland and Antarctica, accompanied by fluctuations in the concentrations of atmospheric carbon dioxide (CO_2) and nitrous oxide (N_2O) as recorded in ice cores. Abrupt changes in the Atlantic Meridional Overturning Circulation (AMOC) have often been invoked to explain the physical characteristics of the D-O oscillations[1], but the mechanisms for the greenhouse gas variations and their linkage to the AMOC have remained unclear[2-5]. Here we present simulations with a coupled model of glacial climate and biogeochemical cycles, forced only with AMOC changes. The model simultaneously reproduces characteristic features of the D-O temperature, CO_2 and N_2O fluctuations. Despite significant changes in land carbon, CO_2 variations on millennial time scales are dominated by slow changes in the deep ocean inventory of biologically-sequestered carbon and are correlated to

Antarctic temperature and Southern Ocean stratification. In contrast, N_2O co-varies more rapidly with Greenland temperatures due to fast adjustments of the thermocline oxygen budget. The results suggest that ocean circulation changes were the primary mechanism that drove glacial CO_2 and N_2O fluctuations on millennial time scales, underscoring the importance of ocean biogeochemistry for projections of future climate change.

Our model simulates the coupled ocean-atmosphere-sea ice-biosphere system[6], including a dynamic terrestrial vegetation and carbon cycle model[7] and a three-dimensional ocean general circulation model with ocean ecosystem dynamics and cycling of nitrogen, phosphorous, oxygen and carbon. The model uses a simple, energy-balance atmosphere and was run under glacial conditions (methods). The model is forced by varying idealized freshwater perturbations to the North Atlantic (Figure 1), mimicking surrounding ice sheet fluctuations. We note that the simulations are idealized, in that the true forcing behind D-O cycles remains unknown. The model forcing is thus arbitrary and was chosen only to trigger AMOC variations.

In response to the forcing, sinking of North Atlantic Deep Water (NADW) stops and the AMOC rapidly spins down from 13 Sv (1 Sv = 10^6 m^3/s) at model year 0 to almost 0 Sv after 100 years. Five sensitivity experiments have been conducted to assess the influence of the duration of the AMOC oscillations. In four experiments the AMOC is switched back on after 400, 700, 1100 and 1700 years, respectively. In one experiment it remains turned off (black lines, Figure 1). The modeled climatic response, including rapid cooling

in the North Atlantic and gradual warming in the Southern Hemisphere, is caused by reduced northward heat transport in the Atlantic as described in detail elsewhere[8]. It is qualitatively consistent with reconstructions but quantitatively underestimates the surface air temperature changes over Greenland and Antarctica, presumably owing to missing atmospheric dynamics. The experiments were not designed to reproduce any particular observed event. We choose D-O event 12 for the comparison in Figure 2 because the duration of the preceding stadial phase corresponds well to one of our experiments.

After the AMOC collapse (following year 0), marine N_2O production rapidly decreases by 40% to less than 1.8 Tg N/yr during year 600 (Figure 1). Figure 3 shows that N_2O production decreases almost everywhere in the global ocean except for the North Atlantic. The decrease is largest in the low oxygen regions of the eastern tropical Pacific and the northern Indian Ocean, but it is also noticeable in the North Pacific and elsewhere. Decreased productivity[9] and better ventilation of thermocline waters lead to increasing subsurface oxygen concentrations, reducing Indo-Pacific N_2O production[10]. Simulated N_2O concentrations co-vary strongly with Greenland temperatures with little time lag (~100 years), consistent with the paleo record[11]. Modeled N_2O amplitudes are 15-40 ppbv, and larger over longer stadials. This is in excellent agreement with ice core data[11] (Figure 2, inset) and consistent with the earlier finding of ref ([11]) that N_2O increase is larger for longer interstadials. The amplitude of our N_2O simulation is much larger than that found in a previous study (10 ppbv) using a zonally averaged ocean model[5]. As noted above, the simulated N_2O production changes show a strong zonal structure and, together with the non-linear dependence of N_2O production on oxygen concentrations, suggest

that a zonally averaged model leads to a systematically biased underestimate. Sensitivity tests showed that the simulated amplitude is insensitive (< 5%) to parameter uncertainties within their 1σ range of the empirical N_2O production equation[12], and that it is only moderately sensitive to the glacial ratio of marine to terrestrial N_2O production. Decreasing this ratio from 1/3 to 1/4 causes only a 15% reduction of the N_2O amplitude.

Methane variations on millennial time scales testify to changes in terrestrial systems during D-O events[13], which presumably also altered N_2O production rates to some degree. However, the history of N_2O changes recorded in ice cores is markedly different than that of methane[11], and the fact that our model can reproduce the correct amplitude of the glacial N_2O variations shows that changes in ocean sources could have dominated glacial variability of atmospheric N_2O on millennial time scales, obviating the need to invoke changes in the terrestrial N_2O source[11,14].

The simulations also resolve a puzzling feature of the N_2O observations. Ref. [11] notes that for long D-O oscillations N_2O begins to increase *before* the rapid warming in Greenland, suggesting a lead and potentially a causal relationship for the AMOC resumptions. The simulations show a comparable lead, but our experimental set-up precludes N_2O effects on climate and hence N_2O variations cannot influence the model AMOC. Rather, the recovery of N_2O is related to the long-term adjustment of the upper ocean nitrate and oxygen inventories after the AMOC collapse. After the initial decrease, upper ocean nutrient levels and global productivity climb after year 600 (not shown), followed

closely by N_2O production. Most of this increase occurs in the North Atlantic and Arctic oceans, as nutrient inventories in these basins slowly adjust to the altered circulation.

In contrast to N_2O, simulated CO_2 concentrations increase slowly by about 25 ppmv, on a millennial time scale, after the AMOC shut down (Figure 1) and decrease again only after the AMOC has resumed, co-varying strongly with Antarctic temperature and ventilation in the Southern Ocean[15]. Despite an increase in terrestrial carbon on a millennial time scale, atmospheric CO_2 increases due to a larger-amplitude decrease in the marine carbon inventory (Figure S1 in the supplementary material). This occurs through a reduction in the global efficiency of the oceanic biological pump, a mechanism which can be most clearly understood through the change in the ocean preformed nutrient inventory[16]. When surface waters in regions with high nutrient concentrations – principally the Southern Ocean – sink into the ocean interior, the capacity of those unutilized (preformed) nutrients to sequester carbon via the biological pump goes unrealized (Fig. S2). In contrast, when nutrient-depleted waters from the subtropical Atlantic flow north to sink as NADW, they entrain relatively little preformed nutrients, thereby encouraging a higher efficiency of the biological pump[17]. A recently proposed theory quantitatively links atmospheric CO_2 changes to changes in the preformed fraction P_{pref}/P_{tot} of the global nutrient inventory [18] , $\Delta pCO_2 = 312 \text{ ppmv} \cdot \Delta P_{pref}/P_{tot}$ (see methods).
P_{pref}/P_{tot} is closely correlated to pCO_2 in our simulations (Fig. 1), increasing from 62% to more than 72% on a millennial time scale. The simple theory yields pCO_2 changes of ~30 ppmv, somewhat overestimating the changes simulated by the complex model. The discrepancy arises mostly from simulated changes in land carbon C_L, which decreases

during the first 250 years, giving rise to the rapid initial increase in atmospheric CO_2 by 5 ppmv, before reversing sign to gradually dampen the long term pCO_2 increase (Fig. S1). We note that the response of C_L is model-dependent, with pronounced sensitivities to atmospheric forcing and the background climate[2,3,19], therefore remaining uncertain. In contrast, the regularity of the relationship between pCO_2 and Southern Ocean temperatures through multiple D-O events gives strong support to our oceanic mechanism, which is relatively insensitive to background climate state. The response time of C_L to the rapid atmospheric forcing in the order of decades to centuries[2,3,19] and thus much shorter than that of the ocean. Thus, the millennial time scale of the observed pCO_2 variations indicates an oceanic mechanism. Our model does not simulate wind changes and associated precipitation variations. Related vegetation changes, particularly in the tropics due to shifts of the intertropical convergence zone are therefore not represented in our simulations. In the future, carbon isotope measurements on pCO_2 might provide more direct constraints on the histories of oceanic versus terrestrial carbon pools.

During the simulated shutdown of the AMOC, two factors conspire to cause the decreased efficiency of the biological pump, both of which relate to the volumetric contributions of water mass end-members to the ocean interior. First, diminished input of low-preformed nutrient NADW to the deep ocean causes the ocean interior to gradually become more dominated by the high-preformed nutrient waters of the Southern Ocean. Second, weakened Southern Ocean stratification, caused by reduced input of salt to the deep waters via NADW, allows more rapid production of waters with high preformed

nutrients[15]. A reviewer (R. Toggweiler) speculated that this could provide a key piece in the puzzle of glacial-interglacial pCO_2 change in the framework of ref ([20]) by illustrating a mechanism for recurring small (~25 ppmv) pCO_2 variations. These could have then produced the full glacial-interglacial cycles through their interaction with the long term adjustment between terrestrial weathering, volcanic CO_2 release, and calcium carbonate sedimentation. Indeed, the modeled sequence of events arising from the AMOC shutdown is consistent with deep ocean chemistry variations during the first deglacial stadial-interstadial oscillation (Heinrich Event 1 and Bolling-Allerod)[21].

Modeled pCO_2 variations (Fig. 1) are ~25 ppmv for long D-O oscillations, consistent with ice core data[22,23], and smaller for shorter oscillations in agreement with previous results[15]. The simulation of small-amplitude pCO_2 changes during short DO oscillations, which are likely to have been more influenced by terrestrial processes, cannot currently be evaluated because of the coarse time resolution of available pCO_2 data, but may be testable in the future as higher resolution data become available[22]. However, the simulated decrease of pCO_2 after the abrupt warming in Greenland is clearly faster than observed (Figure 2, see also ref. [22]). This discrepancy points to processes not captured by the model such as the impact of wind shift induced precipitation changes on vegetation and land carbon storage[2] and/or ocean-sediment interactions, and indicates that more work needs to be done in order to fully reproduce the observed evolution of glacial CO_2 fluctuations on millennial time scales.

The simulations point to an important mechanistic contrast between the oceanic control on these two greenhouse gases, explaining how contrasting atmospheric histories[11,22] can be generated through a unified oceanic process. pCO_2 gradually increases after the interstadial-stadial transition owing to release of carbon from the intermediate and deep ocean related to changes in the global effectiveness of the biological pump[15]. The stadial decrease of N_2O, on the other hand, is much faster because it is controlled by adjustments of upper-ocean oxygen cycling. Our results emphasize the role of ocean circulation and biogeochemical cycling for atmospheric greenhouse gas concentrations. Given model projections of slowing AMOC[24], suggestions that the current ocean sink for carbon is already decreasing[25] and that the ocean source of N_2O might be increasing in the future[6] , further progress in understanding ocean biogeochemical cycles will be required in order to refine the quantification of climate sensitivity to anthropogenic forcing.

REFERENCES

1 Broecker, W. S., Peteet, D. R., and Rind, D., Does the ocean-atmosphere system have more than one stable model of operation? *Nature* **315**, 21 (1985).

2 Menviel, L., A. Timmermann, A. Mouchet, and O. Timm, Meridional reorganizations of marine and terrestrial productivity during Heinrich events. *Paleoceanogr*. **23**, PA1203 (2008).

3 Kohler, P., Joos, F., Gerber, S., and Knutti, R., Simulated changes in vegetation distribution, land carbon storage, and atmospheric CO2 in response to a collapse of the North Atlantic thermohaline circulation. *Clim. Dyn*. **25** (7-8), 689 (2005);

Scholze, M., Knorr, W., and Heimann, M., Modelling terrestrial vegetation dynamics and carbon cycling for an abrupt climatic change event. *Holocene* **13** (3), 327 (2003).

[4] Marchal, O., Stocker, T. F., and Joos, F., Impact of oceanic reorganizations on the ocean carbon cycle and atmospheric carbon dioxide content. *Paleoceanogr*. **13** (3), 225 (1998).

[5] Goldstein, B., Joos, F., and Stocker, T. F., A modeling study of oceanic nitrous oxide during the Younger Dryas cold period. *Geophys. Res. Lett*. **30** (2) (2003).

[6] Schmittner, A., Oschlies, A., Matthews, H. D., and Galbraith, E. D., Future changes in climate, ocean circulation, ecosystems and biogeochemical cycling simulated for a business-as-usual CO2 emission scenario until year 4000 AD. *Glob. Biogeochem. Cycles* **22**, GB1013 (2008).

[7] Meissner, K. J., Weaver, A. J., Matthews, H. D., and Cox, P. M., The role of land surface dynamics in glacial inception: a study with the UVic Earth System Model. *Clim. Dyn*. **21** (7-8), 515 (2003).

[8] Schmittner, A., Saenko, O. A., and Weaver, A. J., Coupling of the hemispheres in observations and simulations of glacial climate change. *Quat. Sci. Rev*. **22** (5-7), 659 (2003).

[9] Schmittner, A., Decline of the marine ecosystem caused by a reduction in the Atlantic overturning circulation. *Nature* **434** (7033), 628 (2005).

[10] Schmittner, A. et al., Large fluctuations of dissolved oxygen in the Indian and Pacific oceans during Dansgaard-Oeschger oscillations caused by variations of North Atlantic Deep Water subduction. *Paleoceanogr*. **22** (3), Pa3207 (2007).

[11] Fluckiger, J. et al., N2O and CH4 variations during the last glacial epoch: Insight into global processes. *Glob. Biogeochem. Cycles* **18** (1), GB1020 (2004).

[12] Nevison, C., Butler, J. H., and Elkins, J. W., Global distribution of N2O and the Delta N2O-AOU yield in the subsurface ocean. *Glob. Biogeochem. Cycles* **17** (4) (2003).

[13] Blunier, T. and Brook, E. J., Timing of millennial-scale climate change in Antarctica and Greenland during the last glacial period. *Science* **291** (5501), 109 (2001).

[14] Sowers, T., Alley, R. B., and Jubenville, J., Ice core records of atmospheric N2O covering the last 106,000 years. *Science* **301** (5635), 945 (2003).

[15] Schmittner, A., Brook, E. J., and Ahn, J., in *Ocean Circulation: Mechanisms and Impacts - Past and Future Changes of Meridional Overturning*, edited by A. Schmittner, J. C. H. Chiang, and S. R. Hemming (American Geophysical Union, Washington, DC, 2007), Vol. 173, pp. 209.

[16] Sigman, D. M. and Haug, G. H., in *Treatise On Geochemistry*, edited by H. D. Holland and K. K. Turekian (Elsevier Science, 2003), Vol. 6, pp. 491.

[17] Toggweiler, J. R. et al., Representation of the carbon cycle in box models and GCMs - 2. Organic pump. *Glob. Biogeochem. Cycles* **17** (1) (2003).

[18] Ito, T. and Follows, M. J., Preformed phosphate, soft tissue pump and atmospheric CO2. *Journal of Marine Research* **63** (4), 813 (2005).

[19] Obata, Atsushi, Climate-Carbon Cycle Model Response to Freshwater Discharge into the North Atlantic. *J. Clim.* **20** (24), 5962 (2007).

[20] Toggweiler, J. R., Origin of the 100,000-year timescale in Antarctic temperatures and atmospheric CO2. *Paleoceanogr.* **23** (2) (2008).

[21] Galbraith, E. D. et al., Carbon dioxide release from the North Pacific abyss during the last deglaciation. *Nature* **449** (7164), 890 (2007).

[22] Ahn, J. and Brook, E. J., Atmospheric CO2 and climate on millennial time scales during the last glacial period *Science* **in revision** (2008).

[23] Ahn, J. and Brook, E. J., Atmospheric CO2 and climate from 65 to 30 ka BP. *Geophys. Res. Lett.* **34** (10) (2007).

[24] Schmittner, A., Latif, M., and Schneider, B., Model projections of the North Atlantic thermohaline circulation for the 21st century assessed by observations. *Geophys. Res. Lett.* **32** (23), L23710 (2005).

[25] Le Quere, C. et al., Saturation of the Southern Ocean CO2 sink due to recent climate change. *Science* **316** (5832), 1735 (2007).

[26] Andersen, K. K. et al., High-resolution record of Northern Hemisphere climate extending into the last interglacial period. *Nature* **431** (7005), 147 (2004).

[27] EPICA, One-to-one coupling of glacial climate variability in Greenland and Antarctica. *Nature* **444** (7116), 195 (2006).

[28] Indermuhle, A. et al., Atmospheric CO2 concentration from 60 to 20 kyr BP from the Taylor Dome ice core, Antarctica. *Geophys. Res. Lett.* **27** (5), 735 (2000).

Acknowledgements This study was funded by the NSF Marine Geology and Geophysics program grant 0728315-OCE, and the NSF Paleoclimate program grant 0602395-ATM.

Thanks to Jinho Ahn, Ed Brook, Robbie Toggweiler and two anonymous referees for discussions and useful comments on the manuscript.

Figure captions

Figure 1: Model simulations of glacial climate and greenhouse gas fluctuations. The five model sensitivity runs differ in the length of the simulated stadial (cold phase in Greenland). Time series of (from top left) freshwater forcing, AMOC, Greenland surface air temperature (SAT), ocean N_2O production (left scale) and atmospheric N_2O concentration (right scale), global fraction of preformed nutrients (left scale) and corresponding changes in atmospheric pCO_2 according to the simple theory[18], Antarctic SAT, and atmospheric CO_2 simulated by the complex model. Red lines correspond to the simulation shown in Figures 2 and 3.

Figure 2: Example of millennial changes in climate and greenhouse gases as recorded in polar ice cores around DO event 12 (left) in comparison with model simulation (right). Greenland observations include $\delta^{18}O$ [26] (temperature proxy) and N_2O concentrations[11]. Antarctic records include $\delta^{18}O$ (Dronning Maud Land[27], grey, and Byrd[13], black), and CO_2 (Taylor Dome[28]) on the age scale of [23], shifted by 1.7ky in order to synchronize with the NGRIP age scale using the rapid methane increase associated with DO 12. Model output shows imposed North Atlantic freshwater forcing, temperature changes over

Greenland (50 W-30 W, 68 N-78 N), atmospheric CO_2 and N_2O, and surface air temperature over Antarctica (68 S-78 S). Inset panel: amplitude of N_2O changes vs. the duration of corresponding stadials, from two ice core records following[11] (blue), and from four model simulations (orange).

Figure 3: Simulated ocean production of N_2O during the interstadial at year 0 (top), during the stadial at year 600 (center) and the difference (year 600 minus year 0, bottom).

Methods

A two-dimensional (vertically averaged) energy-moisture-balance atmospheric model, including prescribed seasonally varying winds, provides a thermodynamically consistent solution for land-ocean surface conditions, without the computationally-demanding requirements of a complex three dimensional atmosphere. The model is well tested and the ocean biogeochemical tracer distributions are in good agreement with observations when integrated under present-day conditions[6]. In order to improve comparison with the paleo record, we simulate aspects of the glacial climate by prescribing (1) land surface conditions in the presence of northern hemisphere (Laurentide and Fennoscandian) ice sheets[29] (i.e. albedo, topography, no vegetation), and (2) decreasing the outgoing long wave radiation at the top-of-the-atmosphere by 2.4 W/m^2, a simple approximation of reduced atmospheric greenhouse gas concentrations. These changes result in globally averaged surface air being 3 K cooler than in the pre-industrial simulation. This is less than the 4-7 K cooling estimated for the Last Glacial Maximum[30], but consistent with intermediate glacial conditions during Marine Isotope Stage 3 (60-25 ka before present).

Physically forced changes in marine and terrestrial carbon cycles result in a modeled glacial atmospheric CO_2 concentration of 255 ppmv, about 25 ppmv lower than the present-day solution, but significantly higher than the observed glacial concentrations (180-220 ppmv). This discrepancy suggests that processes not included in the model, such as changes in aeolian iron supply and/or interactions with ocean sediments, are important on those longer glacial-interglacial time scales[31]. Here we assume that these processes are not important on millennial time scales.

Marine N_2O production was calculated from simulated oxygen concentrations and oxygen consumption rates using an empirical formula (eq. 8 of ref. [12]) that reflects both nitrification and denitrification pathways of N_2O production. N_2O production increases non-linearly with decreasing oxygen concentrations, with most production in the oxygen-depleted regions of the thermocline in the eastern tropical Pacific and the northern Indian Ocean (Figure 3). The model predicts a global pre-industrial marine N_2O production of 3.7 Tg N/ yr, which is at the lower end of the range of observation based estimates[12,32]. In the 'glacial' simulation, oceanic N_2O production is decreased by 22% to 2.9 Tg N/yr due to increased oxygen solubility in colder water, consistent with marine sediment evidence[33]. Terrestrial N_2O production, which is a poorly-understood function of soil moisture and oxygenation, is not explicitly modeled. Instead, to calculate the effect of changes in marine production on atmospheric N_2O concentrations we assume a constant terrestrial source twice the size of the oceanic source at year 0 (as estimated for present day), a constant atmospheric lifetime of 120 years, initial N_2O concentrations of 250 ppbv, and an instantaneous balance between oceanic and terrestrial sources and the

atmospheric sink. Since we calculate atmospheric N_2O offline its changes do not affect modeled climate (in contrast to CO_2 changes). This is warranted because the radiative effect of the resulting N_2O changes is small.

The remineralized nutrient concentration $P_{remi} = AOU*R_{P:O}$ is estimated from the apparent oxygen utilization $AOU = O_2^{sat} - O_2$, where O_2^{sat} is the temperature dependent oxygen saturation concentration and assuming a constant phosphorous to oxygen ratio $R_{P:O}$. The efficiency of the biological pump can be expressed as the biologically sequestered fraction $P_{remi}/P_{tot} = 1 - P_{pref}/P_{tot}$ of the total nutrient inventory (remineralized nutrients, P_{remi}).

References Methods

[29] Peltier, W. R., Global glacial isostasy and the surface of the ice-age earth: The ice-5G (VM2) model and grace. *Annual Review of Earth and Planetary Sciences* **32**, 111 (2004).

[30] Jansen, E. et al., in *Climate Change 2007: The Physical Science Basis. Contribution of Working Group I to the Fourth Assessment Report of the Intergovernmental Panel on Climate Change*, edited by S. Solomon, D. Qin, M. Manning, Z. Chen, M. Marquis, K.B. Averyt, M. Tignor and H.L. Miller (Cambridge University Press, Cambridge, United Kingdom and New York, NY, USA, 2007).

[31] Brovkin, V., Ganopolski, A., Archer, D., and Rahmstorf, S., Lowering of glacial atmospheric CO2 in response to changes in oceanic circulation and marine

biogeochemistry. *Paleoceanogr*. **22** (4) (2007); Broecker, W. S. and Peng, T. H., The role of CaCO3 compensation in the glacial to interglacial atmospheric CO2 change. *Glob. Biogeochem. Cycles* **1** (1), 15 (1987).

[32] Hirsch, A. I. et al., Inverse modeling estimates of the global nitrous oxide surface flux from 1998-2001. *Glob. Biogeochem. Cycles* **20** (1) (2006).

[33] Meissner, K. J., Galbraith, E. D., and Volker, C., Denitrification under glacial and interglacial conditions: A physical approach. *Paleoceanogr*. **20** (3) (2005); Galbraith, E. D., Kienast, M., Pedersen, T. F., and Calvert, S. E., Glacial-interglacial modulation of the marine nitrogen cycle by high-latitude O-2 supply to the global thermocline. *Paleoceanogr*. **19** (4) (2004).

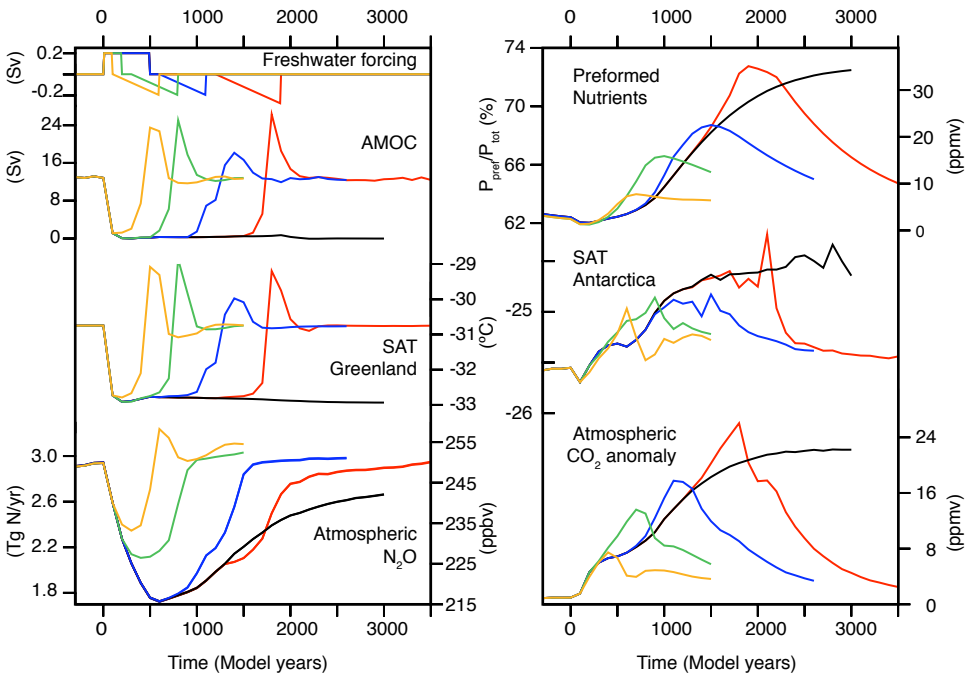
Freshwater forcing
AMOC
SAT
Greenland
Atmospheric
N2O
(Sv)
(Tg N/yr)
(°C)
(ppbv)
Time (Model years)
Preformed
Nutrients
SAT
Antarctica
Atmospheric
CO2 anomaly
Pref/Ptot (%)
(ppmv)
Time (Model years)

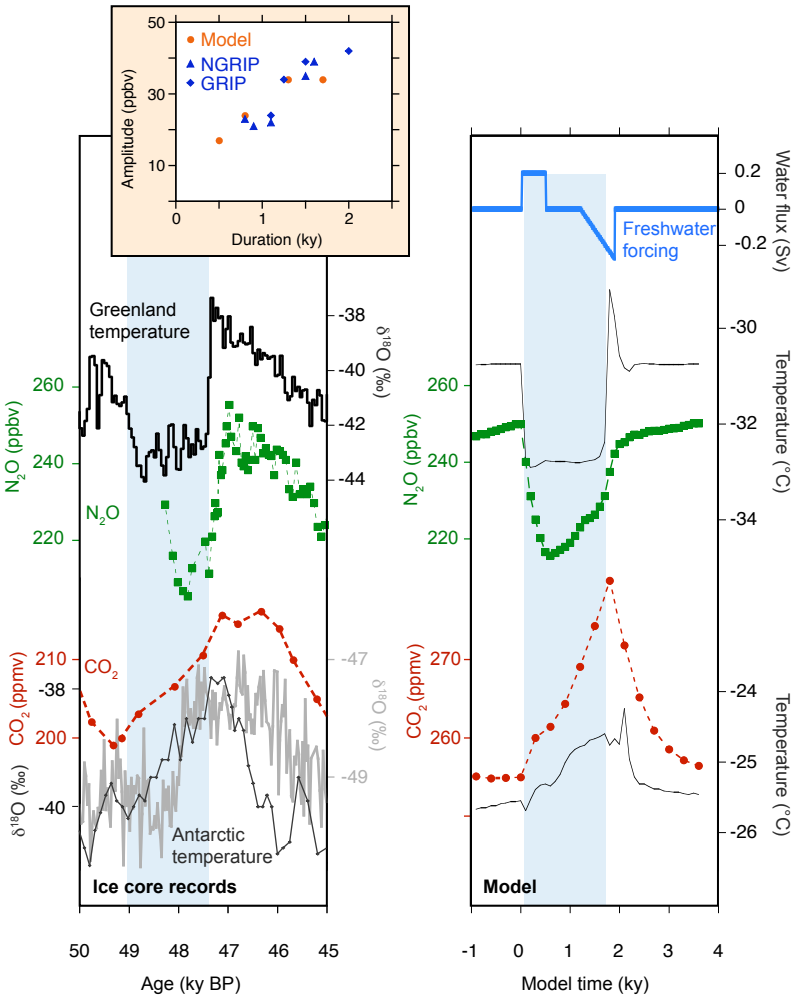
Model
NGRIP
GRIP
Amplitude (ppbv)
Duration (ky)
Greenland temperature
N2O
CO2
Antarctic temperature
Ice core records
N2O (ppbv)
CO2 (ppmv)
δ18O (‰)
Age (ky BP)
Freshwater forcing
Water flux (Sv)
Temperature (°C)
Model
Model time (ky)

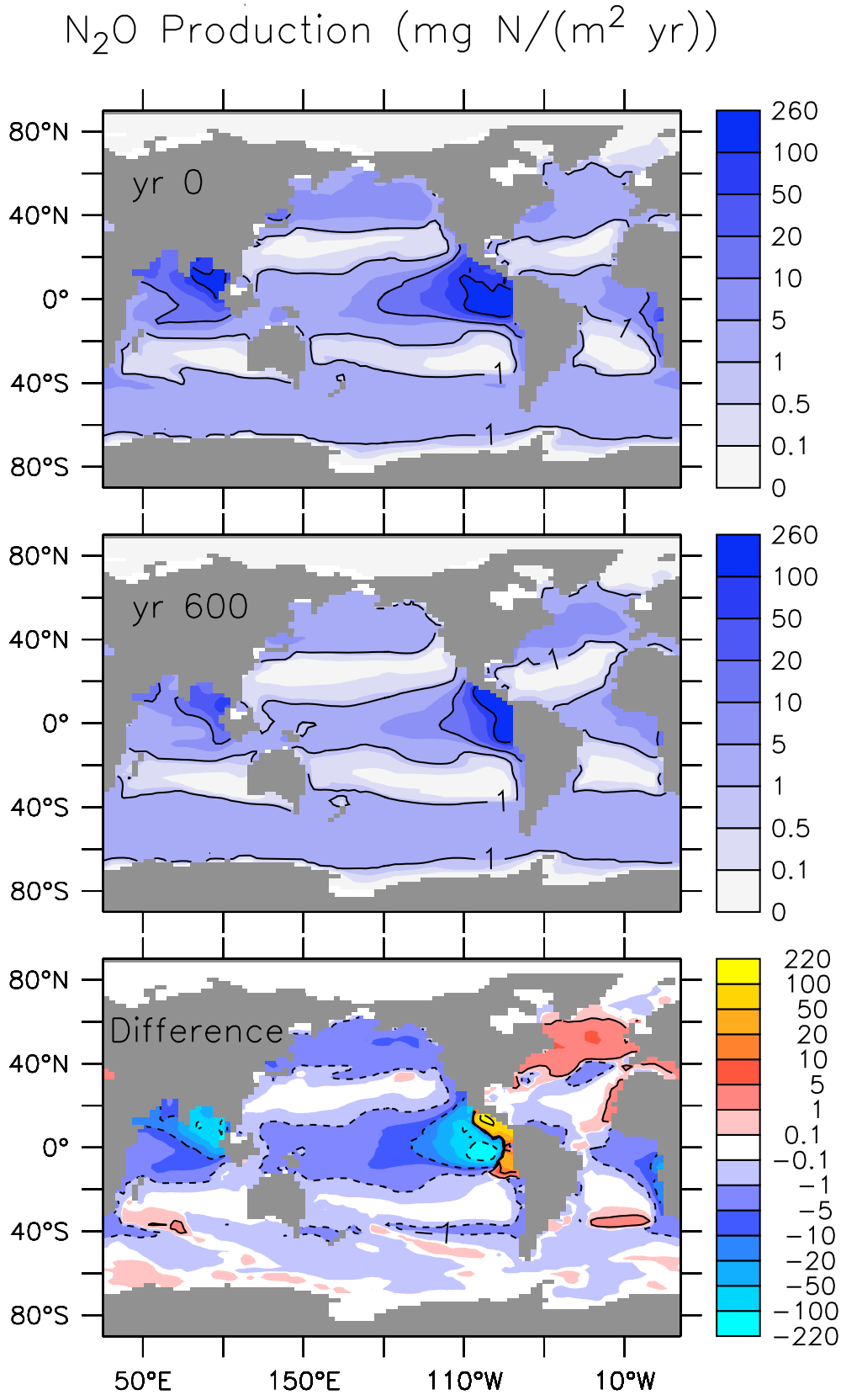
N2O Production (mg N/(m2 yr))
yr 0
yr 600
Difference
80°N
40°N
0°
40°S
80°S
50°E
150°E
110°W
10°W
260
100
50
20
10
5
1
0.5
0.1
0
220
100
50
20
10
5
1
0.1
−0.1
−1
−5
−10
−20
−50
−100
−220